

C-SAW: Self-Supervised Prompt Learning for Image Generalization in Remote Sensing

Avigyan Bhattacharya

Indian Institute of Technology Bombay
Mumbai, Maharashtra, India

Ankit Jha

Indian Institute of Technology Bombay
Mumbai, Maharashtra, India

Mainak Singha

Indian Institute of Technology Bombay
Mumbai, Maharashtra, India

Biplab Banerjee

Indian Institute of Technology Bombay
Mumbai, Maharashtra, India

ABSTRACT

We focus on domain and class generalization problems in analyzing optical remote sensing images, using the large-scale pre-trained vision-language model (VLM), CLIP. While contrastively trained VLMs show impressive zero-shot generalization performance, their effectiveness is limited when dealing with diverse domains during training and testing. Existing prompt learning techniques overlook the importance of incorporating domain and content information into the prompts, which results in a drop in performance while dealing with such multi-domain data. To address these challenges, we propose a solution that ensures domain-invariant prompt learning while enhancing the expressiveness of visual features. We observe that CLIP’s vision encoder struggles to identify contextual image information, particularly when image patches are jumbled up. This issue is especially severe in optical remote sensing images, where land-cover classes exhibit well-defined contextual appearances. To this end, we introduce C-SAW, a method that complements CLIP with a self-supervised loss in the visual space and a novel prompt learning technique that emphasizes both visual domain and content-specific features. We keep the CLIP backbone frozen and introduce a small set of projectors for both the CLIP encoders to train C-SAW contrastively. Experimental results demonstrate the superiority of C-SAW across multiple remote sensing benchmarks and different generalization tasks.

CCS CONCEPTS

• **Computing methodologies** → **Prompt Learning, Self-supervised Learning, Neural Network.**

KEYWORDS

Vision-language models, remote sensing, self-supervised learning, prompt learning

ACM Reference Format:

Avigyan Bhattacharya, Mainak Singha, Ankit Jha, and Biplab Banerjee. 2023. C-SAW: Self-Supervised Prompt Learning for Image Generalization in Remote Sensing. In *Proceedings of 14th Indian Conference on Computer*

Permission to make digital or hard copies of part or all of this work for personal or classroom use is granted without fee provided that copies are not made or distributed for profit or commercial advantage and that copies bear this notice and the full citation on the first page. Copyrights for third-party components of this work must be honored. For all other uses, contact the owner/author(s).

ICVGIP’23, December 2023, Ropar, India

© 2023 Copyright held by the owner/author(s).

ACM ISBN 123-4567-24-567/08/06.

<https://doi.org/10.475/3627631.3627669>

Vision, Graphics and Image Processing (ICVGIP’23). ACM, New York, NY, USA, 10 pages. <https://doi.org/10.475/3627631.3627669>

1 INTRODUCTION

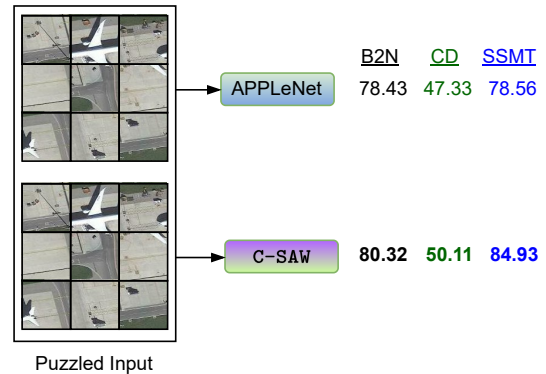


Figure 1: C-SAW shows better performance scores in comparison to APPLeNet [63] for jumbled RS images. Here, B2N, CD and SSMT represent base-to-new class generalization, cross-dataset generalization and single source multi target generalization, respectively.

In recent times, the field of remote sensing (RS) imaging has witnessed remarkable advancements, revolutionizing Earth’s surface monitoring for diverse applications, such as urban planning [27] and environmental monitoring [60]. Representation learning, a common approach in this domain, involves pre-training a model on a large image dataset, like ImageNet [33], using a supervised approach, showcasing significant improvements in various downstream tasks. However, the effectiveness of traditional deep learning models in analyzing complex RS images and outperforming ad-hoc machine learning methods is hampered by challenges in generalization when faced with domain shifts.

To tackle these challenges, researchers have explored the areas of domain adaptation (DA) [21, 72], which entails capturing representations of the target domain during model adaptation, drawing from knowledge obtained from the target distribution during training, and domain generalization (DG) [35, 87] addresses the practical scenario where the inclusion of RS data covering vast diversity during model training becomes arduous. DG capitalizes on labeled data from multiple source domains to learn a versatile and universal representation, striving to build an accurate model that adeptly handles any “unseen” target domain. Despite the resounding success

of DG in the computer vision field, its potential application in the context of RS imagery remains relatively unexplored.

Large multimodal foundation models, such as CLIP [57], ALIGN [29], and ViLBERT [45], have demonstrated impressive performance in downstream tasks, even with limited training data under zero-shot or few-shot learning scenarios. These models establish connections between image and text pairs through contrastive learning and effectively fine-tuning with hand-crafted text prompts. This success has paved the way for two exciting research directions. The first direction focuses on adapting pre-trained VLMs to diverse downstream tasks thus venturing into the area of transfer learning. Popular transfer approaches, such as prompt tuning [31, 63, 88, 89] and visual adaptation [23, 83], also strive to achieve the desired objectives. On the other hand, the second direction explores knowledge distillation [15, 24], enhancing VLMs' performance in downstream tasks like object detection and semantic segmentation. Remote sensing images often face adverse conditions, like high altitudes or cloudiness, making it challenging to classify them using pre-trained CNN models. To address this, APLeNet [63] leverages prompt learning to generalize across remote sensing domains. Additionally, it employs context redundancy penalizing (CRP) loss to reduce redundancy between context tokens.

However, this paper dives into the promising area of self supervised learning, a technique that has garnered popularity due to its accomplishments in language and vision [19, 32, 34, 82]. Self-supervised learning offers an attractive alternate to supervised pre-training, guiding models to learn better embedding spaces. It has the potential to significantly enhance representation learning in RS image analysis, bolstering the generalization capabilities of models across diverse environments. By leveraging self-supervised learning and contrastive methods [9, 10], our work emphasizes the prospects of advancing RS image analysis through domain generalization techniques, contributing to the domain's evolution and yielding valuable insights into RS applications. In order to incorporate the SSL task, we create the patches of the input image and then jumble it before passing through the pre-trained vision encoder to get the contextual latent embeddings.

As CLIP [57] is trained on massive datasets of image-text pairs, it is able to learn the relationship between images and their corresponding text descriptions, thus gaining recognition for its remarkable prowess. *However, despite its success, CLIP encounters a challenge in that it struggles to discern the positional relationships among different parts of an image, leading to occasional difficulties in processing jumbled imagery.* Let us assume a jumbled image where various parts have been intentionally scrambled, presenting a captivating puzzle for CLIP to solve. In such intriguing scenarios, VLMs are not able to rely solely on its pre-trained knowledge to identify distinct part embeddings of the image. Unfortunately, acquiring sufficient data for fine-tuning a VLM to conquer this challenge is not always feasible.

In remote sensing data for computer vision, dealing with scrambled satellite images poses a unique challenge. These images have parts out of order due to practical factors like data transmission errors or limitations in satellite imaging. Using pretrained CLIP directly on such jumbled images is difficult as the extracted features lack meaningful information. APLeNet [63] has achieved

significant performance gains over CLIP and other learning methods for domain generalization in remote sensing images. However, APLeNet encounters difficulties when dealing with jumbled RS images. As shown in Figure 1, our demonstrations indicate that APLeNet's performance decreases by approximately 0.2% - 0.8% on average across three types of domain generalization tasks (Base-to-New, Cross Dataset, and Single Source Multi Target) when presented with jumbled RS images instead of non-jumbled ones. To address this challenge of handling jumbled RS data effectively, we propose a method called C-SAW. It leverages a contrastive self-supervised learning framework for robust domain generalization. Through a context-aware self-supervision mechanism, we divide an image into smaller patches and rearrange them randomly. With SSL training involving reconstruction and self-supervised loss, our approach reconstructs the original image while learning robust contextual representations from the jigsaw inputs. These learned representations enable the model to efficiently perform diverse downstream tasks, including classification. In summary, our contributions are as follows:

- We propose a novel self-supervised prompt learning technique called C-SAW for image generalization in remote sensing applications.
- Our proposed method, C-SAW, tackles the limitations of part embeddings in CLIP by incorporating a reconstruction task to enhance the latent visual space of the distorted input image. Furthermore, we generate the visual attention tokens using $\mathcal{G}_{V,AT}$ before the frozen text encoder in CLIP to impose desired prompt constraints on the input visual embeddings.
- We extensively tested our approach on five optical remote sensing (RS) image classification benchmarks, evaluating its performance on three challenging generalization tasks: cross-dataset, base-to-new class, and single-source multi-target. Our results demonstrate that C-SAW surpasses the relevant literature by a significant margin, achieving a mean classification score improvement of approximately 2-6%.

2 RELATED WORKS

2.1 Self-Supervised Learning in Remote Sensing

Stojnic et al. in [64, 65] apply split-brain autoencoders [84] and Contrastive Multiview Coding (CMC) [69] on aerial images to learn effective representations for classification tasks while SatMAE [13] uses a masked autoencoder modified for remote sensing data. Recent works in semantic segmentation include [38] with a global style-local matching contrastive learning approach and [48] for the Vaihingen dataset. FALSE [85] proposes efficient negative sampling, where as [2, 42] addresses supervision noise and temporal alignment. Other contrastive approaches include [68], where they use SSL approach to obtain high performance pre-training and [30], where the authors make use of the semantic similarities among nearby scenes. [74] creates diverse samples through spatial and spectral transformations. GAN discriminators are used in [16] and [11] for temporal and multiview images, respectively. For detailed information, one can refer to [67, 77].

2.2 Domain Generalization

One of the crucial tasks for deep learning models facing domain shift challenges between training and test distributions, which is mainly referred to as *domain generalization* task. This task encompasses mainly two variants: multi-source domain generalization (Multi-DG) and single-source domain generalization (Single-DG). In Multi-DG, researchers have explored *meta learning* approaches [20, 35] and subsequent works have built upon this, incorporating it for regularizers, semantic consistency, and feature critic losses [4, 18, 44]. *Adversarial training* methods [39, 43, 49] and *Domain augmentation* techniques [6, 61, 80, 90, 91] have been adopted to align feature distributions across different domains and generate new domains through adversarial examples. Other methods address Multi-DG through domain-specific masks, gradient-based dropout, episodic training, and style bias reduction techniques [8, 28, 36, 51]. Over the years, Single-DG has gained more attention as a practical and challenging problem. Domain expansion is a prevalent approach in this regard, [40, 55, 56, 76, 78, 79, 86] although different methods have also been proposed, including adversarial attacks with semantic restrictions, information bottleneck techniques, Wasserstein auto-encoders, contrastive learning, uncertainty estimation, and objective functions for domain expansion [40, 55, 56, 66, 70, 71, 76, 79, 86]. Despite these efforts, domain generalization for remote sensing (RS) image classification remains an area with limited attention to date [52, 87].

2.3 Vision-Language Models and Prompt Learning

Large-scale Vision-Language Models (VLMs) fuse visual and textual inputs, enhancing performance in various computer vision tasks. Multimodal learning excels over unimodal approaches in feature learning, benefiting tasks like visual question answering (VQA) [1], image captioning [75], and image retrieval [3], which rely on joint visual-semantic supervision. VLMs typically employ pre-trained language models like BERT [14] and GPT [58] for textual encoding, while Convolutional Networks (ConvNets) or Vision Transformers process visual inputs. Notable VLMs include CLIP [57] and VisualBERT [41].

Prompt learning gained popularity in NLP [53] and visual recognition tasks, utilizing pre-trained language models like BERT to offer valuable information through textual prompts for downstream tasks. Automated prompt generation, explored in AutoPrompt [62], identifies tokens with significant gradient changes for prompt optimization. CoOp [89] fine-tunes CLIP for few-shot image classification, optimizing prompts, whereas other methods, like ProGrad [92], generate prompts from visual features and optimize context tokens. Additionally, PDL [47] proposes optimizing multiple prompt sets.

In the domain generalization for remote sensing images, APLeNet [63] introduces a vision-language prompting technique. SLIP [50] improves CLIP's performance by supplementing contrastive learning with a self-supervised learning objective in a multi-task setup. These methods showcase the growing interest in prompt learning to enhance language models' capabilities in visual recognition tasks.

CoCoOp [88] focuses on learning text prompts conditioned to input image embeddings, facilitating more context-aware queries. ProGrad [92] employs prompt tuning through distillation, transferring knowledge from learned few-shot prompts to zero-shot prompts, which can be especially valuable for improving generalization. MaPLe [31] specializes in fine-tuning the CLIP model by aligning vision and text modalities, enhancing the model's overall performance. APLeNet [63] leverages attention mechanisms on conditioned image embeddings to improve text-prompting, simultaneously minimizing redundancy between context vectors for more efficient text conditioning on images. In contrast, C-SAW introduces a novel approach, that showcases the effectiveness of CLIP over *image part embeddings by incorporating a reconstruction task (SSL)* to enhance the latent visual space of distorted input images. Additionally, it generates visual attention tokens to impose desired prompt constraints on the input visual embeddings.

3 PROBLEM DEFINITION & METHODOLOGY

We define dataset $\mathcal{D} = \{\mathcal{D}_S \cup \mathcal{D}_T\}$, where \mathcal{D}_S and \mathcal{D}_T represent the source and target domains, respectively, with each domain containing input data \mathcal{X} and corresponding labels \mathcal{Y} . The probability distributions $P(\mathcal{D}_S^i)$ can vary for each domain. During training, we utilize labels \mathcal{Y}_S from the source domains \mathcal{D}_S , while during testing, our focus shifts to labels \mathcal{Y}_T from a distinct target test domain \mathcal{D}_T . The probability distribution $\mathcal{P}(\mathcal{D}_T)$ differs from $\mathcal{P}(\mathcal{D}_S^i) \forall i$. For base-to-new class generalization, there is no overlap between the label sets \mathcal{Y}_S and \mathcal{Y}_T . In single-source domain generalization, the label sets are identical, resulting in $\mathcal{Y}_S \cap \mathcal{Y}_T = \mathcal{Y}_S \cup \mathcal{Y}_T$. The cross-dataset domain generalization presents variable situations of overlapping or non-overlapping label sets, warranting further exploration. This analysis provides valuable insights into domain adaptation and the relationships between source and target domains in diverse generalization scenarios.

3.1 The Proposed C-SAW:

In our paper, we introduce C-SAW, a novel approach that enhances text token learning and leverages the effectiveness of CLIP's visual backbone with jumbled input images (x') as presented in Figure 2. The pre-trained CLIP's vision encoder f_v extracts features from both the original input image (x) and the jumbled input image (x'), enabling contrastive generalization of images with text embeddings from the pre-trained CLIP's text encoder f_t . To achieve domain-agnostic style features for domain generalization, we utilize the mean μ of a batch of features from the intermediate layers ($\mathcal{I}\mathcal{L}$) of CLIP's vision encoder. We observed that CLIP faces challenges in generalizing classification tasks when generating prompts from part-embeddings of x' . To overcome this, our proposed C-SAW generates visual attentive tokens using $\mathcal{G}_{V, \mathcal{A}\mathcal{T}}$. Additionally, we optimize C-SAW using the following losses; \mathcal{L}_{ce} for classification, \mathcal{L}_{dm} for contextualizing pre-trained CLIP's vision encoder for generalizing over part-embeddings of jumbled input images, and \mathcal{L}_{ssl} for self-supervised learning to improve generalization. Furthermore, we use \mathcal{L}_{recon} to reconstruct the original image from the jumbled input image, which helps in strengthening the latent space of x' . In the following subsections, we provide detailed explanations of our key contributions.

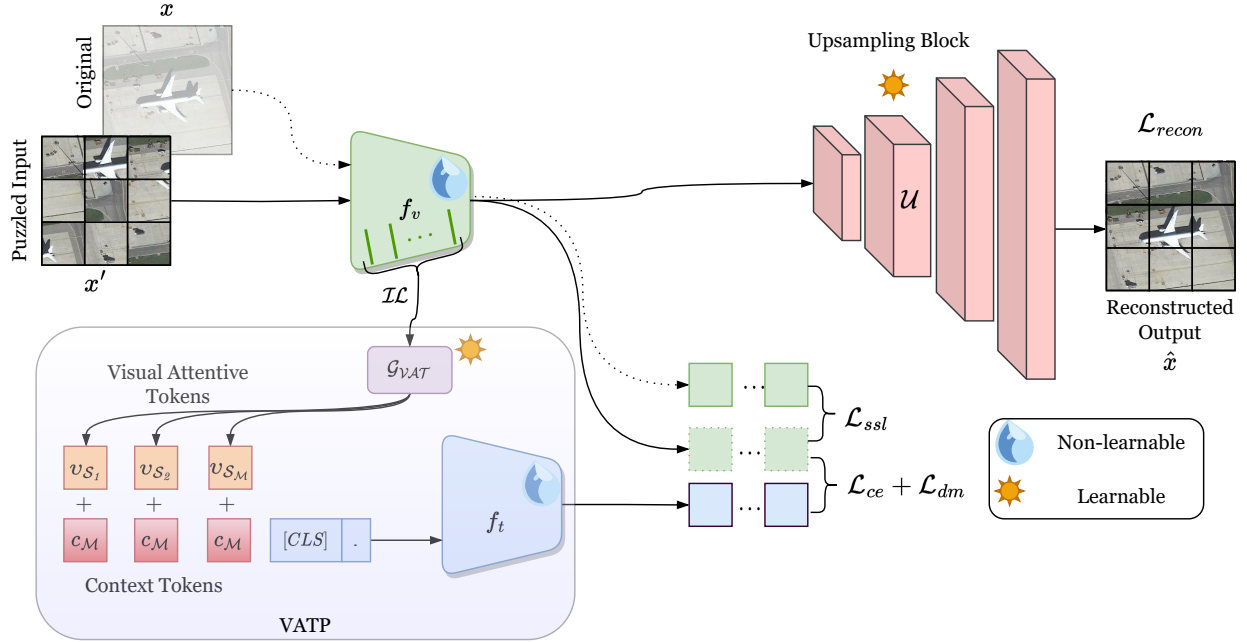


Figure 2: Our proposed C-SAW architecture utilizes f_v and f_t as the visual and text encoders, respectively, from CLIP’s frozen backbone. The visual attentive token generator \mathcal{G}_{VAT} generates M visual attentive tokens v_S using intermediate layers $\mathcal{I}\mathcal{L}$ of the source domains \mathcal{S} . These visual attentive tokens, along with context and class tokens, create text embeddings using f_t , forming the visual attentive text prompting (VATP) approach. We utilize these final image-conditioned prompt embeddings for the classification task under the supervision of the cross-entropy loss (\mathcal{L}_{ce}). Additionally, the upsampling block \mathcal{U} , represented in light pink, is associated with the reconstruction loss \mathcal{L}_{recon} , self-supervised loss (\mathcal{L}_{ssl}), and diversity maximization loss (\mathcal{L}_{dm}). Best viewed in colour.

Self-supervised Block: We propose an upsampling network (\mathcal{U}) to upscale the jigsaw or jumbled visual features from the vision encoder $f_v(x')$, aiming to reconstruct the original image x . Our upsampling network (\mathcal{U}) consists of four convolutional (CNN) layers, where the output dimensions of the first three CNN layers are reduced by half of the input dimensions using a kernel size of 7, a stride of 3, padding of 1, and output padding of 2. The channel dimension of the last CNN layer is set to match the input channel dimension of the RGB image. Finally, we reshape the output of the last layer through bilinear interpolation to match the shape of the original images, i.e., $\mathcal{U}(f_v(x')) = \hat{x} \in \mathbb{R}^{3 \times 224 \times 224}$.

We further strengthen the contextualizing ability of CLIP’s vision encoder f_v part embeddings, using self-supervision between visual features $f_v(x')$ and $f_v(x)$. We define the reconstruction and self-supervised losses, i.e., \mathcal{L}_{recon} and \mathcal{L}_{ssl} , in the subsequent paragraphs.

Visual Attentive Text Prompting (VATP): We derive the style representation for each domain by averaging the feature statistics μ of each batch B from the respective domain. These statistics are obtained from the intermediate layers $\mathcal{I}\mathcal{L}$ of the visual encoder of pre-trained CLIP. The style representation for the i^{th} source domain is denoted as μ_{S_i} . The generative visual attentive token \mathcal{G}_{VAT} block takes the style information μ_S to generate M attentive tokens v_{S_M} conditioned on the input image x . Mathematically, this is

denoted as $v_{S_M} = \mathcal{G}_{VAT}(\mu(x'))$. The \mathcal{G}_{VAT} block consists of n linear layers, each for extracting style features from n intermediate layers f_v^l , where $l \in \{1, \dots, n\}$ and $f_v^l \in \mathbb{R}^{W \times H \times C}$ with W , H and C denote height, width and channel, respectively.

To generate the visual attentive tokens, we first create an attention mask $A(f_v^l(x')) = \text{sign}(\mathcal{G}_{VAT}(f_v^l(x')))$ by passing the obtained style features through a two-layer bottleneck structure, Linear-ReLU-Linear-Sigmoid. We then multiply and add this attention mask with the style features $f_v^l(x')$ in a residual manner to obtain the M visual attentive tokens v_{S_M} , which is defined as

$$v_{S_M}(x') = [A(f_v^l(x')) \odot f_v^l(x')] + f_v^l(x') \quad (1)$$

These visual attentive tokens $v_{S_M}(x')$ are combined with textual tokens c_M , i.e., $\tilde{c}_M(x') = c_M + v_{S_M}(x')$. Finally, they pass through CLIP’s pretrained text encoder f_t to obtain the prompt token embeddings $\text{prompt}_{emb}(x')$, mathematically defined as

$$\text{prompt}_{emb}(x') = f_t(\tilde{c}_M(x')) \in \mathbb{R}^{K \times 512} \quad (2)$$

Where K denotes the number of classes. We follow the same process on the original input image x to obtain $\text{prompt}_{emb}(x)$. Finally, we compute the average of both prompt embeddings:

$$\text{APE}(x', x) = \text{prompt}_{emb_{avg}}(x', x) = \frac{\text{prompt}_{emb}(x') + \text{prompt}_{emb}(x)}{2} \quad (3)$$

which allowing us to perform the classification contrastively with the visual feature of x' , i.e., $f_v(x')$.

3.2 Losses and Network Optimization

Cross-entropy Loss: We classify the jumbled images (x') of the original images (x) in the contranstrive manner with average text prompts generated with the respective conditioned input images i.e., $APE(x', x)$. The prediction probability for x' to belong to the label y is denoted by,

$$p(y|x') = \frac{\exp(\langle f_v(x'), APE(x', x) \rangle / \tau)}{\sum_{k=1}^{|\mathcal{Y}|} \exp(\langle f_v(x'), APE(x', x) \rangle / \tau)} \quad (4)$$

Here, $\langle \cdot \rangle$ represents the cosine similarity, while τ stands for the temperature hyper-parameter. To compute the cross-entropy loss (\mathcal{L}_{ce}), we compare the prediction probabilities of each input image with their corresponding class labels as follows:

$$\mathcal{L}_{ce} = \arg \min_{\mathcal{G}_{V, \mathcal{A}, \mathcal{T}}} \mathbb{E}_{(x', x, y) \in \mathcal{P}(\mathcal{D}_s)} - \sum_{k=1}^{\mathcal{Y}_s} y_k \log(p(y_k|x')) \quad (5)$$

Self-supervised Loss: We integrate BARLOW TWINS self-supervision [81] to align features from $f_v(x')$ and $f_v(x)$, vision encoders for jumbled and original images, name as \mathcal{L}_{ssl} . This objective minimizes the discrepancy between cross-correlation and identity matrices, resulting in similar embeddings for distorted samples, removing redundancy. Our approach improves feature learning, leading to more coherent and efficient representations.

Reconstruction Loss: To achieve better peak signal-to-noise ratio between the jigsaw puzzle images (x') and reconstructed images ($\hat{x} = \mathcal{U}(f_v(x'))$), we incorporate the l_2 -norm between which is defined as,

$$\mathcal{L}_{recon} = \arg \min_{\mathcal{U}} \mathbb{E}_{\mathcal{P}(\mathcal{D}_s)} \|\hat{x} - x'\|_2 \quad (6)$$

Diversity Maximization Loss: Additionally, we enforce a limitation on the similarity distribution between the visual features $f_v(x')$ of the target samples and prompt embeddings, by minimizing the entropy of prediction probabilities. It is defined as,

$$\mathcal{L}_{dm} = \arg \min_{p(y|x')} \mathbb{E}_{\mathcal{P}(\mathcal{D}_s)} \min([p(y_1|x'); \dots; p(y_{|\mathcal{Y}|}|x')]) \quad (7)$$

Total Loss: We optimize our proposed C-SAW with total loss, \mathcal{L}_{total} is computed as:

$$\mathcal{L}_{total} = \arg \min_{p(y|x'), \mathcal{U}, \mathcal{G}_{V, \mathcal{A}, \mathcal{T}}} [\mathcal{L}_{ce} + \alpha * (\mathcal{L}_{ssl} + \mathcal{L}_{recon}) + (1 - \alpha) * \mathcal{L}_{dm}] \quad (8)$$

where α is a weight ratio factor associated for optimally balancing the ssl and diversity maximization losses.

4 EXPERIMENTAL RESULTS

Datasets: For our experiments, we have used five remote sensing benchmark datasets i.e. PatternNet [37], RSICD [46], RESISC45 [12], MLRSNet [54] and EuroSat [26]. The PatternNet dataset comprises 38 classes, with each class consisting of 800 images sized (256×256) pixels. RSICD contains 30 classes and a total of 10,000 images, each with a size of 224×224 pixels. It's important to note that each

class within RSICD has a varying number of images. The RESISC45 dataset consists of 45 classes, with each class containing 700 images sized (256×256) pixels. MLRSNet, on the other hand, comprises 46 classes and a total of 109,161 images, each sized (256×256) pixels. The Eurosat consists of 10 classes with total 27,000 geo-referenced images.

Additionally, we also work on generating learnable prompts within the single-source multi-target (SSMT) domain generalization setups, as mentioned in APPLeNet [63]. The mentioned curated dataset consists of 16 overlapping classes that are common across all four datasets and suits for domain generalization tasks.

Implementation Details: We implemented our method in PyTorch on a 12GB Nvidia RTX 3090-Ti GPU card. Our proposed C-SAW is trained for 50 epochs using stochastic gradient descent (SGD) optimizer [59]. The initial learning rate is set to $2e^{-4}$ with a warm-up fixed rate of $1e^{-7}$ to prevent explosive gradients. Input images are rescaled to (224×224) pixels and fed into CLIP's frozen encoder (ViT-B/16 [17]) for a latent dimension of \mathbb{R}^{512} . The model is trained with 16 samples per class and a batch size of 4. We experimentally choose the α values to be in between $[0.5, 0.7]$, shown in Figure 3.

To initialize text prompts, we use "a photo of a [CLS]" embeddings, following previous literature [63, 88, 89], resulting in a context length of four. Three different seeds are used for evaluation, and the average top-1 accuracy is reported. We experimentally select the parameters for optimizer, input preprocessing, and prompt initialization for optimal learning and convergence our proposed C-SAW.

4.1 Comparison

In this section, we conduct a thorough comparison between our novel approach, C-SAW, and existing methods in the realm of deep learning. We assess their performance across three different domain generalization (DG) tasks: **Base-to-Novel (B2N) Class Generalization:** This task involves training and testing the model on separate sets of classes without any overlap between them. **Cross-Dataset (CD) Generalization:** Here, the model is trained on one dataset and then tested on new datasets that have variations in both their domains and labels. **Single Source Multi-Target (SSMT) Domain Generalization:** In this task, the model is trained on a specific source domain and then evaluated on multiple new domains, all within a closed-set scenario. To evaluate the effectiveness of our proposed C-SAW, we compare it against several established techniques, including zero-shot (ZS) CLIP [57], ERM [73], and DANN [22] for the SSMT task. Furthermore, we benchmark C-SAW against state-of-the-art (SOTA) prompt learning methods like CoOp [89], CoCoOp [88], CLIP-Adapter [23], ProGrad [92], MaPLe [31], APPLeNet [63] and StyLIP [5], which serve as **baseline** methods for all the generalization tasks under consideration.

B2N class generalization: Table 1 presents the experimental results for Base-to-Novel (B2N) class generalization across five remote sensing (RS) datasets. The Table 1 includes the computation of the harmonic mean (HM), which represents the balance between the classification accuracies of the base and novel classes. For defining

the source and target domains, we randomly and equally divide each dataset into two groups. We compare the performance of C-SAW with optimization-based methods that rely on referred context. Our proposed C-SAW method outperforms SOTA methods on the PatternNet, RSICD, RESISC45, MLRSNet and EuroSat datasets by margins of at least 3.5%, 1.3%, 2.0%, 3.1%, and 1.3% respectively, when considering the harmonic mean of base and novel classes. Among the preferred methods, MaPLe shows significant performances over the non-RS methods and holds the third-best performance. APLeNet achieves the second-best performance in generalizing the unseen classes across all RS datasets. However, when compared to CLIP’s zero-shot approach, C-SAW demonstrates superior generalization scores, with a substantial margin of 37.33% for seen classes and 10.18% for unseen classes averaged across all the remote sensing datasets.

The impressive performance gains of C-SAW in the B2N class generalization tasks highlight its effectiveness in adapting to novel classes in remote sensing datasets. The results reinforce C-SAW’s capability to achieve robust domain generalization across diverse RS datasets and outperform existing optimization-based and zero-shot approaches. These findings position C-SAW as a competitive and reliable solution for class generalization in remote sensing domain adaptation tasks.

CD generalization: In the cross-dataset setup, we have evaluated C-SAW on the PatternNet dataset (source domain), and zero-shot inference results were reported for the remaining remote sensing (RS) datasets (target domains), as shown in Table 2. Our method demonstrates remarkable improvements in both source and target classification performance. It surpasses zero-shot CLIP by substantial margins of 27.2% in the source domain and 4.46% on average across the target domains. Moreover, C-SAW outperforms SOTA methods by at least 2.55% on average across the unseen target datasets. These results highlight the effectiveness of C-SAW in reducing the generalization gap between a single source and multiple target domains, even in the presence of domain and label shifts, within the CD generalization technique. The significant performance gains achieved by C-SAW in the CD setup underscore its ability to generalize effectively across diverse and unseen RS datasets. This demonstrates its potential for practical applications in remote sensing domain generalization tasks, where models must perform well on previously unseen target domains. The superior performance of C-SAW compared to zero-shot CLIP and other SOTA methods further solidifies its position as a promising approach for domain generalization and transfer learning in the remote sensing domain.

SSMT domain generalization: In the Single-Source Multi-Target (SSMT) domain generalization setup, which differs from the previously discussed cross-dataset transfer (CDT) setting with shared classes across domains, we select the PatternNetv2 dataset as the target domain, following the approach of APLeNet [63]. The results presented in Table 3 demonstrate the remarkable performance of C-SAW. Our proposed method has outperformed all the SOTA methods, showcasing a substantial lead of at least 4.67% on RSICDv2, 5.35% on RESISC45v2, and 4.23% on the MLRSNetv2 datasets. Overall, C-SAW exhibited notably superior performance, achieving a

4.94% improvement over the average performance across the target domains. The performance superiority of C-SAW in the SSMT setup further validates its effectiveness in addressing the domain generalization challenges in remote sensing images. These results underscore the potential of our approach in real-world applications, where adapting to diverse and unseen target domains is crucial. The robust performance gains achieved by C-SAW across multiple target domains highlight its promise as a practical and effective solution for remote sensing domain generalization tasks.

4.2 Ablation Studies

Ablation study on weight ratio factor (α): In this section, we have investigated the impact of the weight ratio factor (α) on the performance of our model, C-SAW. α determines the balance between self-supervision and supervision tasks that C-SAW should carry to optimize its performance, as defined by Eq. 8, where α and $(1 - \alpha)$ represent the ratios in which the two tasks are involved, respectively. Figure 3 illustrates the results of varying the weight ratio factor α . We have observed that the best performance is achieved when $\alpha = 0.5$, particularly in the B2N and SSMT setups. For the CD setup, the optimal weight ratio factor is found to be $\alpha = 0.7$. These findings indicate that striking an appropriate balance between self-supervision and supervision tasks is critical to maximizing the performance of C-SAW across different experimental setups. By fine-tuning the weight ratio factor, we ensure that C-SAW effectively leverages both forms of training signals, leading to superior performance in domain generalization tasks.

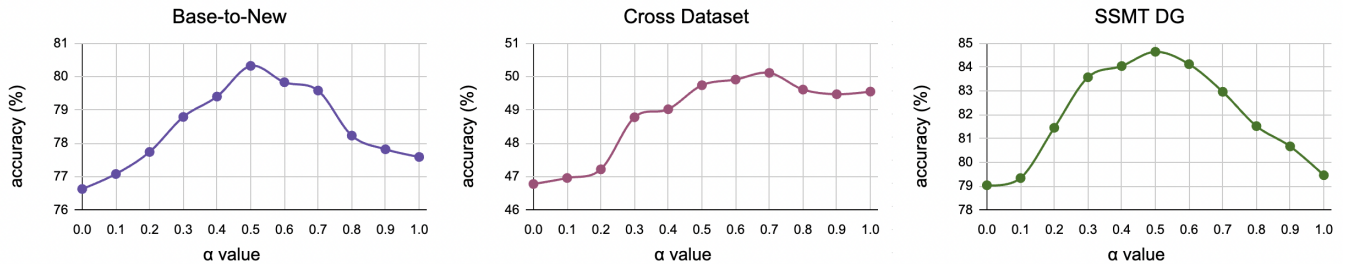
Evaluation of C-SAW’s sensitivity to the number of shots: The performance of our proposed C-SAW is assessed by varying the number of shots from 1 to all for the B2N class generalization task. A comparison is made against SOTA prompting techniques, as presented in Table 4. For this evaluation, we utilize a context length of 4, position the class token at the end, employ ViT-B/16 [17] as the visual feature backbone, and utilize a unified context vector. Since CLIP operates in a zero-shot manner, it is excluded from this comparison, and we focus solely on few-shot-based prompting methods while showcasing results on the average of all RS datasets. Our results demonstrate that C-SAW surpasses the performance of benchmark prompt learning-based methods by at least 1.9%, 2.2%, 2.3%, 2.4% and 2.1% for 1, 4, 8, 16 shots and all images, respectively.

Ablation study on loss terms: We have performed several experiments with our proposed model, C-SAW, employing different loss terms, as outlined in Table 5. One of these loss terms, *SSL* defines the self-supervision importance of the model. It combines the self-supervised loss (\mathcal{L}_{ssl}) and reconstruction loss (\mathcal{L}_{recon}). They are commonly used to minimize the gap between self-supervised views and the original images. By taking only these losses with \mathcal{L}_{ce} , decreases the model performance by 2.73%, 0.56% and 5.18% in B2N, CD and SSMT set up respectively. For that reason, we have considered a *Non-SSL* loss \mathcal{L}_{dm} . However, considering \mathcal{L}_{dm} only and removing *SSL* losses lead to a performance decrease of 3.69%, 3.33% and 5.60% in B2N, CD and SSMT set up respectively. From Eq. 8, here we have considered when $\alpha = 1.0$, only *SSL* loss works, when $\alpha = 0$, only \mathcal{L}_{dm} contributes and when $\alpha = 0.5$, the best

Table 1: Comparing C-SAW with SOTA methods on base-to-new class generalization over existing methods on 5 different remote sensing datasets on 16-shots with context length, $M=4$. HM represents the harmonic mean.

(a) Average over 5 datasets				(b) PatternNet				(c) RSICD			
Method	Base	New	HM	Method	Base	New	HM	Method	Base	New	HM
CLIP [57]	56.50	60.04	58.22	CLIP [57]	63.67	64.37	64.02	CLIP [57]	54.61	55.33	54.97
CoOp [89]	89.65	57.34	69.94	CoOp [89]	91.62	62.23	74.12	CoOp [89]	92.52	56.08	69.83
CLIP-Adt [23]	81.94	59.05	68.64	CLIP-Adt [23]	82.15	63.26	71.48	CLIP-Adt [23]	78.93	55.44	65.13
CoCoOp [88]	87.71	59.02	70.56	CoCoOp [88]	92.39	63.34	75.16	CoCoOp [88]	93.18	58.67	72.00
ProGrad [92]	87.55	51.18	64.60	ProGrad [92]	92.65	62.48	74.63	ProGrad [92]	93.44	58.15	71.69
MaPLe [31]	90.85	63.11	74.48	MaPLe [31]	94.74	66.12	77.88	MaPLe [31]	94.91	60.52	73.91
APPLeNet [63]	90.95	63.72	74.94	APPLeNet [63]	94.89	65.57	77.55	APPLeNet [63]	95.26	60.71	74.16
StyLIP [5]	91.25	63.51	74.90	StyLIP [5]	95.13	66.78	78.47	StyLIP [5]	94.98	60.92	74.23
C-SAW	92.90	66.03	77.20	C-SAW	96.03	70.18	81.09	C-SAW	95.13	62.56	75.48

(d) RESISC45				(e) MLRSNet				(f) EuroSAT			
Method	Base	New	HM	Method	Base	New	HM	Method	Base	New	HM
CLIP [57]	56.32	55.38	55.85	CLIP [57]	51.43	51.92	51.67	CLIP [57]	56.48	64.05	60.03
CoOp [89]	89.04	55.75	68.57	CoOp [89]	75.21	53.64	62.62	CoOp [89]	92.19	57.74	68.69
CLIP-Adt [23]	81.67	56.23	66.60	CLIP-Adt [23]	71.64	53.19	61.05	CLIP-Adt [23]	85.28	61.07	71.17
CoCoOp [88]	89.78	57.18	69.86	CoCoOp [88]	76.32	52.75	62.38	CoCoOp [88]	87.49	60.04	71.21
ProGrad [92]	90.13	57.89	70.50	ProGrad [92]	75.96	52.23	61.90	ProGrad [92]	87.04	44.67	59.04
MaPLe [31]	91.45	60.82	73.05	MaPLe [31]	79.06	54.85	64.59	MaPLe [31]	94.07	73.23	82.35
APPLeNet [63]	91.24	60.46	72.73	APPLeNet [63]	78.53	56.41	65.66	APPLeNet [63]	94.81	75.46	84.04
StyLIP [5]	90.87	60.34	72.52	StyLIP [5]	80.65	55.47	65.73	StyLIP [5]	94.61	74.06	83.08
C-SAW	92.56	62.70	74.76	C-SAW	85.41	57.52	68.74	C-SAW	95.39	77.20	85.33

**Figure 3: Ablation of weight ratio factor (α) in all generalization setup.****Table 2: Comparing C-SAW with SOTA methods for cross-dataset generalization with PatternNet dataset as the source domain and remaining RS datasets as the target domains.**

Method	Source		Target				Average
	PatternNet	RSICD	RESISC45	MLRSNet	EuroSAT		
CLIP [57]	61.72	43.25	48.56	45.13	43.24	45.65	
CoOp [89]	85.23	42.53	49.34	44.50	46.51	45.46	
CLIP-Adapter [23]	74.27	42.57	49.07	44.17	44.75	45.27	
CoCoOp [88]	85.95	43.61	49.53	44.72	46.82	45.95	
ProGrad [92]	86.14	41.25	48.26	44.12	45.97	44.54	
MaPLe [31]	87.92	45.23	49.56	46.37	47.63	47.05	
APPLeNet [63]	88.17	44.87	50.97	46.83	49.52	47.56	
StyLIP [5]	88.01	46.12	49.89	46.94	49.79	48.19	
C-SAW	88.92	50.47	50.60	49.26	50.54	50.11	

Table 3: Comparing C-SAW with SOTA methods for single-source multi-target domain generalization on the benchmark RS datasets.

Method	Source		Target			Average
	PatternNetv2	RSICDv2	RESISC45v2	MLRSNetv2		
ERM [73]	73.69	61.40	61.59	61.13	61.37	
CLIP [57]	78.04	72.15	75.42	67.78	71.78	
DANN [22]	93.56	75.49	76.18	70.53	74.07	
CoOp [89]	94.25	76.50	77.87	70.97	75.11	
CLIP-Adapter [23]	92.36	79.17	79.76	71.04	76.66	
CoCoOp [88]	94.41	79.33	80.43	71.67	77.14	
ProGrad [92]	95.18	77.46	80.65	72.29	76.80	
MaPLe [31]	96.52	80.45	83.37	76.15	79.99	
APPLeNet [63]	96.63	81.03	82.23	74.03	79.10	
StyLIP [5]	96.85	80.67	84.56	75.66	80.30	
C-SAW	97.91	85.70	88.72	80.38	84.93	

output comes for B2N and SSMT DG tasks as discussed above in details on the importance of α factor.

Table 4: Comparing C-SAW with the SOTA methods on varying the number of shots for the B2N class generalization (considered harmonic mean HM) task with average of all RS datasets.

Method	1-shot	4-shot	8-shot	16-shot	All
CoOp [89]	65.31	66.85	67.52	69.94	67.68
CLIP-Adapter [23]	63.40	64.58	67.11	68.64	66.57
CoCoOp [88]	66.82	68.31	69.03	70.56	68.85
ProGrad [92]	59.33	61.16	63.44	64.60	60.86
MaPLe[31]	73.42	74.28	76.63	77.49	76.72
APLeNet[63]	75.82	76.23	77.69	78.43	78.51
C-SAW	77.14	77.83	79.42	80.32	79.95

Table 5: Ablation study of C-SAW with different settings of losses in all generalization setup over average of all RS datasets. Here, we define SSL ($\mathcal{L}_{ssl} + \mathcal{L}_{recon}$).

Loss	B2N	CD	SSMT
\mathcal{L}_{ce}	72.93	45.82	76.39
$\mathcal{L}_{ce} + SSL$	77.59	49.55	79.46
$\mathcal{L}_{ce} + \mathcal{L}_{dm}$	76.63	46.78	79.04
$\mathcal{L}_{ce} + SSL + \mathcal{L}_{dm}$	80.32	50.11	84.64

Ablation study on context lengths: The context length four "a photo of a [CLS]" is common and experimentally found to be optimal in SOTA prompt-learning methods [31, 88, 92]. As shown in Table 6, we have experimented and found that the context length of 4 provides best performance in comparison with $M = 8, 12$ and 16.

Table 6: Comparing C-SAW with the SOTA methods on varying context length for the B2N class generalization.

Context Length (M)	4	8	12	16
C-SAW	80.32	79.55	79.02	77.39

Table 7: Comparing C-SAW with different feature extractors for single-source multi-target domain generalization on the benchmark RS datasets.

Method	Source		Target		
	PatternNetv2	RSICDv2	RESISC45v2	MLRSNetv2	Average
RN50[25]	65.12	54.30	52.77	53.45	53.51
DINO[7]	80.55	74.10	71.92	75.39	73.80
C-SAW	97.91	85.70	88.72	80.38	84.93

Ablation study on feature extractors: Since CLIP is the most popular SOTA for few-shot or zero-shot tasks in computer vision, we use CLIP as the frozen network for feature extractor and perform prompt tuning for various downstream tasks. We also compare our proposed C-SAW with simple vision extractors like *ResNet-50* (RN50) [25] and *DINO* [7] on SSMT DG task, and we can clearly observe that prompt learning conditioned to image features outperforms pre-trained feature extractors at least by 11% as mentioned in Table 7.

5 CONCLUSIONS

We present C-SAW, a framework designed to enhance the multi-domain generalization capability of CLIP-derived features by introducing two key improvements on top of the frozen CLIP model. Firstly, we propose a jigsaw-based self-supervised objective to supplement CLIP's vision encoder. This addition injects the importance of part-aware visual feature learning, effectively addressing a limitation present in the baseline CLIP model. Secondly, we introduce a novel prompt learning approach within C-SAW, strategically integrating visual content and style primitives into the prompts. This integration enables the model to achieve better generalization to previously unseen domains and classes. Through these innovative modifications, C-SAW demonstrates impressive performance in dealing with challenging optical remote sensing images, by achieving better generalization across diverse domains and classes. In the future, we aim to further enhance the model's capabilities by incorporating outlier identification ability, unlocking even more potential for anomaly detection and handling challenging scenarios.

REFERENCES

- [1] Aishwarya Agrawal, Jiasen Lu, Stanislaw Antol, Margaret Mitchell, C. Lawrence Zitnick, Dhruv Batra, and Devi Parikh. 2016. VQA: Visual Question Answering. arXiv:1505.00468 [cs.CL]
- [2] Kumar Ayush, Burak Uzkent, Chenlin Meng, Kumar Tanmay, Marshall Burke, David Lobell, and Stefano Ermon. 2021. Geography-aware self-supervised learning. In *Proceedings of the IEEE/CVF International Conference on Computer Vision*. 10181–10190.
- [3] Artem Babenko, Anton Slesarev, Alexandr Chigorin, and Victor Lempitsky. 2014. Neural codes for image retrieval. In *European conference on computer vision*. Springer, 584–599.
- [4] Yogesh Balaji, Swami Sankaranarayanan, and Rama Chellappa. 2018. Metareg: Towards domain generalization using meta-regularization. *Advances in neural information processing systems* 31 (2018).
- [5] Shirsha Bose, Enrico Fini, Ankit Jha, Mainak Singha, Biplab Banerjee, and Elisa Ricci. 2023. StyLIP: Multi-Scale Style-Conditioned Prompt Learning for CLIP-based Domain Generalization. *arXiv preprint arXiv:2302.09251* (2023).
- [6] Fabio Maria Carlucci, Paolo Russo, Tatiana Tommasi, and Barbara Caputo. 2019. Hallucinating agnostic images to generalize across domains. In *2019 IEEE/CVF International Conference on Computer Vision Workshop (ICCVW)*. IEEE, 3227–3234.
- [7] Mathilde Caron, Hugo Touvron, Ishan Misra, Hervé Jégou, Julien Mairal, Piotr Bojanowski, and Armand Joulin. 2021. Emerging properties in self-supervised vision transformers. In *Proceedings of the IEEE/CVF international conference on computer vision*. 9650–9660.
- [8] Prithvijit Chattopadhyay, Yogesh Balaji, and Judy Hoffman. 2020. Learning to balance specificity and invariance for in and out of domain generalization. In *Computer Vision—ECCV 2020: 16th European Conference, Glasgow, UK, August 23–28, 2020, Proceedings, Part IX* 16. Springer, 301–318.
- [9] Ting Chen, Simon Kornblith, Mohammad Norouzi, and Geoffrey Hinton. 2020. A simple framework for contrastive learning of visual representations. In *International conference on machine learning*. PMLR, 1597–1607.
- [10] Xinlei Chen, Haoqi Fan, Ross Girshick, and Kaiming He. 2020. Improved baselines with momentum contrastive learning. *arXiv preprint arXiv:2003.04297* (2020).
- [11] Yuxing Chen and Lorenzo Bruzzone. 2021. Self-supervised change detection by fusing SAR and optical multi-temporal images. In *2021 IEEE International Geoscience and Remote Sensing Symposium IGARSS*. IEEE, 3101–3104.
- [12] Gong Cheng, Junwei Han, and Xiaoqiang Lu. 2017. Remote sensing image scene classification: Benchmark and state of the art. *Proc. IEEE* 105, 10 (2017), 1865–1883.
- [13] Yezhen Cong, Samar Khanna, Chenlin Meng, Patrick Liu, Erik Rozi, Yutong He, Marshall Burke, David Lobell, and Stefano Ermon. 2022. Satmae: Pre-training transformers for temporal and multi-spectral satellite imagery. *Advances in Neural Information Processing Systems* 35 (2022), 197–211.
- [14] Jacob Devlin, Ming-Wei Chang, Kenton Lee, and Kristina Toutanova. 2018. Bert: Pre-training of deep bidirectional transformers for language understanding. *arXiv preprint arXiv:1810.04805* (2018).
- [15] Jian Ding, Nan Xue, Gui-Song Xia, and Dengxin Dai. 2022. Decoupling zero-shot semantic segmentation. In *Proceedings of the IEEE/CVF Conference on Computer Vision and Pattern Recognition*. 11583–11592.

- [16] Huihui Dong, Wenping Ma, Yue Wu, Jun Zhang, and Licheng Jiao. 2020. Self-supervised representation learning for remote sensing image change detection based on temporal prediction. *Remote Sensing* 12, 11 (2020), 1868.
- [17] Alexey Dosovitskiy, Lucas Beyer, Alexander Kolesnikov, Dirk Weissenborn, Xiaohua Zhai, Thomas Unterthiner, Mostafa Dehghani, Matthias Minderer, Georg Heigold, Sylvain Gelly, Jakob Uszkoreit, and Neil Houlsby. 2020. An Image is Worth 16x16 Words: Transformers for Image Recognition at Scale. *CoRR abs/2010.11929* (2020). arXiv:2010.11929 <https://arxiv.org/abs/2010.11929>
- [18] Qi Dou, Daniel Coelho de Castro, Konstantinos Kamnitsas, and Ben Glocker. 2019. Domain generalization via model-agnostic learning of semantic features. *Advances in Neural Information Processing Systems* 32 (2019).
- [19] Hongchao Fang, Sicheng Wang, Meng Zhou, Jiayuan Ding, and Pengtao Xie. 2020. Cert: Contrastive self-supervised learning for language understanding. *arXiv preprint arXiv:2005.12766* (2020).
- [20] Chelsea Finn, Pieter Abbeel, and Sergey Levine. 2017. Model-agnostic meta-learning for fast adaptation of deep networks. In *International conference on machine learning*. PMLR, 1126–1135.
- [21] Yaroslav Ganin and Victor Lempitsky. 2015. Unsupervised domain adaptation by backpropagation. In *International conference on machine learning*. PMLR, 1180–1189.
- [22] Yaroslav Ganin, Evgeniya Ustinova, Hana Ajakan, Pascal Germain, Hugo Larochelle, François Laviolette, Mario Marchand, and Victor Lempitsky. 2016. Domain-adversarial training of neural networks. *The journal of machine learning research* 17, 1 (2016), 2096–2030.
- [23] Peng Gao, Shijie Geng, Renrui Zhang, Teli Ma, Rongyao Fang, Yongfeng Zhang, Hongsheng Li, and Yu Qiao. 2021. Clip-adapter: Better vision-language models with feature adapters. *arXiv preprint arXiv:2110.04544* (2021).
- [24] Xiuye Gu, Tsung-Yi Lin, Weicheng Kuo, and Yin Cui. 2021. Open-vocabulary object detection via vision and language knowledge distillation. *arXiv preprint arXiv:2104.13921* (2021).
- [25] Kaiming He, Xiangyu Zhang, Shaoqing Ren, and Jian Sun. 2016. Deep residual learning for image recognition. In *Proceedings of the IEEE conference on computer vision and pattern recognition*. 770–778.
- [26] Patrick Helber, Benjamin Bischke, Andreas Dengel, and Damian Borth. 2019. Eurosat: A novel dataset and deep learning benchmark for land use and land cover classification. *IEEE Journal of Selected Topics in Applied Earth Observations and Remote Sensing* 12, 7 (2019), 2217–2226.
- [27] Miyuki Hino, Elinor Benami, and Nina Brooks. 2018. Machine learning for environmental monitoring. *Nature Sustainability* 1, 10 (2018), 583–588.
- [28] Zeyi Huang, Haohan Wang, Eric P Xing, and Dong Huang. 2020. Self-challenging improves cross-domain generalization. In *Computer Vision—ECCV 2020: 16th European Conference, Glasgow, UK, August 23–28, 2020, Proceedings, Part II* 16. Springer, 124–140.
- [29] Chao Jia, Yinfei Yang, Ye Xia, Yi-Ting Chen, Zarana Parekh, Hieu Pham, Quoc Le, Yun-Hsuan Sung, Zhen Li, and Tom Duerig. 2021. Scaling up visual and vision-language representation learning with noisy text supervision. In *International Conference on Machine Learning*. PMLR, 4904–4916.
- [30] Jian Kang, Ruben Fernandez-Beltran, Puhong Duan, Sicong Liu, and Antonio J Plaza. 2020. Deep unsupervised embedding for remotely sensed images based on spatially augmented momentum contrast. *IEEE Transactions on Geoscience and Remote Sensing* 59, 3 (2020), 2598–2610.
- [31] Muhammad Uzair Khattak, Hanoona Rasheed, Muhammad Maaz, Salman Khan, and Fahad Shahbaz Khan. 2023. MaPLe: Multi-Modal Prompt Learning. In *Proceedings of the IEEE/CVF Conference on Computer Vision and Pattern Recognition (CVPR)*. 19113–19122.
- [32] Alexander Kolesnikov, Xiaohua Zhai, and Lucas Beyer. 2019. Revisiting self-supervised visual representation learning. In *Proceedings of the IEEE/CVF conference on computer vision and pattern recognition*. 1920–1929.
- [33] Alex Krizhevsky, Ilya Sutskever, and Geoffrey E Hinton. 2012. Imagenet classification with deep convolutional neural networks. *Advances in neural information processing systems* 25 (2012).
- [34] Zhenzhong Lan, Mingda Chen, Sebastian Goodman, Kevin Gimpel, Piyush Sharma, and Radu Soricut. 2019. Albert: A lite bert for self-supervised learning of language representations. *arXiv preprint arXiv:1909.11942* (2019).
- [35] Da Li, Yongxin Yang, Yi-Zhe Song, and Timothy Hospedales. 2018. Learning to generalize: Meta-learning for domain generalization. In *Proceedings of the AAAI conference on artificial intelligence*, Vol. 32.
- [36] Da Li, Jianshu Zhang, Yongxin Yang, Cong Liu, Yi-Zhe Song, and Timothy M Hospedales. 2019. Episodic training for domain generalization. In *Proceedings of the IEEE/CVF International Conference on Computer Vision*. 1446–1455.
- [37] Hongzhi Li, Joseph G Ellis, Lei Zhang, and Shih-Fu Chang. 2018. Patternnet: Visual pattern mining with deep neural network. In *Proceedings of the 2018 ACM on international conference on multimedia retrieval*. 291–299.
- [38] Haifeng Li, Yi Li, Guo Zhang, Ruoyun Liu, Haozhe Huang, Qing Zhu, and Chao Tao. 2022. Global and local contrastive self-supervised learning for semantic segmentation of HR remote sensing images. *IEEE Transactions on Geoscience and Remote Sensing* 60 (2022), 1–14.
- [39] Haoliang Li, Sinno Jialin Pan, Shiqi Wang, and Alex C Kot. 2018. Domain generalization with adversarial feature learning. In *Proceedings of the IEEE conference on computer vision and pattern recognition*. 5400–5409.
- [40] Lei Li, Ke Gao, Juan Cao, Ziyao Huang, Yepeng Weng, Xiaoyue Mi, Zhengze Yu, Xiaoya Li, and Boyang Xia. 2021. Progressive domain expansion network for single domain generalization. In *Proceedings of the IEEE/CVF Conference on Computer Vision and Pattern Recognition*. 224–233.
- [41] Liunian Harold Li, Mark Yatskar, Da Yin, Cho-Jui Hsieh, and Kai-Wei Chang. 2019. Visualbert: A simple and performant baseline for vision and language. *arXiv preprint arXiv:1908.03557* (2019).
- [42] Wenyan Li, Keyan Chen, Hao Chen, and Zhenwei Shi. 2021. Geographical knowledge-driven representation learning for remote sensing images. *IEEE Transactions on Geoscience and Remote Sensing* 60 (2021), 1–16.
- [43] Ya Li, Xinmei Tian, Mingming Gong, Yajing Liu, Tongliang Liu, Kun Zhang, and Dacheng Tao. 2018. Deep domain generalization via conditional invariant adversarial networks. In *Proceedings of the European conference on computer vision (ECCV)*. 624–639.
- [44] Yiying Li, Yongxin Yang, Wei Zhou, and Timothy Hospedales. 2019. Feature-critic networks for heterogeneous domain generalization. In *International Conference on Machine Learning*. PMLR, 3915–3924.
- [45] Jiasen Lu, Dhruv Batra, Devi Parikh, and Stefan Lee. 2019. Vilbert: Pretraining task-agnostic visiolinguistic representations for vision-and-language tasks. *Advances in neural information processing systems* 32 (2019).
- [46] Xiaoqiang Lu, Binqiang Wang, Xiangtao Zheng, and Xuelong Li. 2017. Exploring models and data for remote sensing image caption generation. *IEEE Transactions on Geoscience and Remote Sensing* 56, 4 (2017), 2183–2195.
- [47] Yuning Lu, Jianzhuang Liu, Yonggang Zhang, Yajing Liu, and Xinmei Tian. 2022. Prompt distribution learning. In *Proceedings of the IEEE/CVF Conference on Computer Vision and Pattern Recognition*. 5206–5215.
- [48] Valerio Marsocci, Simone Scardapane, and Nikos Komodakis. 2021. MARE: Self-supervised multi-attention REsu-Net for semantic segmentation in remote sensing. *Remote Sensing* 13, 16 (2021), 3275.
- [49] Toshihiko Matsuura and Tatsuya Harada. 2020. Domain generalization using a mixture of multiple latent domains. In *Proceedings of the AAAI Conference on Artificial Intelligence*, Vol. 34. 11749–11756.
- [50] Norman Mu, Alexander Kirillov, David Wagner, and Saining Xie. 2022. Slip: Self-supervision meets language-image pre-training. In *Computer Vision—ECCV 2022: 17th European Conference, Tel Aviv, Israel, October 23–27, 2022, Proceedings, Part XXVII*. Springer, 529–544.
- [51] Hyeonseob Nam, HyunJae Lee, Jongchan Park, Wonjun Yoon, and Donggeun Yoo. 2021. Reducing domain gap by reducing style bias. In *Proceedings of the IEEE/CVF Conference on Computer Vision and Pattern Recognition*. 8690–8699.
- [52] Claudio Persello and Lorenzo Bruzzone. 2014. Relevant and invariant feature selection of hyperspectral images for domain generalization. In *2014 IEEE Geoscience and Remote Sensing Symposium*. IEEE, 3562–3565.
- [53] Fabio Petroni, Tim Rocktäschel, Patrick Lewis, Anton Bakhtin, Yuxiang Wu, Alexander H Miller, and Sebastian Riedel. 2019. Language models as knowledge bases? *arXiv preprint arXiv:1909.01066* (2019).
- [54] Xiaoman Qi, Panpan Zhu, Yuebin Wang, Liqiang Zhang, Junhuan Peng, Mengfan Wu, Jialong Chen, Xudong Zhao, Ning Zang, and P Takis Mathiopoulos. 2020. MLRSNet: A multi-label high spatial resolution remote sensing dataset for semantic scene understanding. *ISPRS Journal of Photogrammetry and Remote Sensing* 169 (2020), 337–350.
- [55] Fengchun Qiao and Xi Peng. 2021. Uncertainty-guided model generalization to unseen domains. In *Proceedings of the IEEE/CVF conference on computer vision and pattern recognition*. 6790–6800.
- [56] Fengchun Qiao, Long Zhao, and Xi Peng. 2020. Learning to learn single domain generalization. In *Proceedings of the IEEE/CVF Conference on Computer Vision and Pattern Recognition*. 12556–12565.
- [57] Alec Radford, Jong Wook Kim, Chris Hallacy, Aditya Ramesh, Gabriel Goh, Sandhini Agarwal, Girish Sastry, Amanda Askell, Pamela Mishkin, Jack Clark, et al. 2021. Learning transferable visual models from natural language supervision. In *International Conference on Machine Learning*. PMLR, 8748–8763.
- [58] Alec Radford, Karthik Narasimhan, Tim Salimans, Ilya Sutskever, et al. 2018. Improving language understanding by generative pre-training. (2018).
- [59] Herbert Robbins and Sutton Monro. 1951. A stochastic approximation method. *The annals of mathematical statistics* (1951), 400–407.
- [60] Floyd F Sabins. 1999. Remote sensing for mineral exploration. *Ore geology reviews* 14, 3–4 (1999), 157–183.
- [61] Shiv Shankar, Vihari Piratla, Soumen Chakrabarti, Siddhartha Chaudhuri, Preethi Jyothi, and Sunita Sarawagi. 2018. Generalizing across domains via cross-gradient training. *arXiv preprint arXiv:1804.10745* (2018).
- [62] Taylor Shin, Yasaman Razeghi, Robert L Logan IV, Eric Wallace, and Sameer Singh. 2020. Autoprompt: Eliciting knowledge from language models with automatically generated prompts. *arXiv preprint arXiv:2010.15980* (2020).
- [63] Mainak Singha, Ankit Jha, Bhupendra Solanki, Shirsha Bose, and Biplab Banerjee. 2023. APPLENet: Visual Attention Parameterized Prompt Learning for Few-Shot Remote Sensing Image Generalization Using CLIP. In *Proceedings of the IEEE/CVF*

- Conference on Computer Vision and Pattern Recognition (CVPR) Workshops*. 2023–2033.
- [64] Vlada Stojnić and Vladimir Risojević. 2018. Evaluation of split-brain autoencoders for high-resolution remote sensing scene classification. In *2018 International Symposium ELMAR*. IEEE, 67–70.
- [65] Vlada Stojnić and Vladimir Risojević. 2021. Self-supervised learning of remote sensing scene representations using contrastive multiview coding. In *Proceedings of the IEEE/CVF Conference on Computer Vision and Pattern Recognition*. 1182–1191.
- [66] Christian Szegedy, Wojciech Zaremba, Ilya Sutskever, Joan Bruna, Dumitru Erhan, Ian Goodfellow, and Rob Fergus. 2013. Intriguing properties of neural networks. *arXiv preprint arXiv:1312.6199* (2013).
- [67] Chao Tao, Ji Qi, Mingning Guo, Qing Zhu, and Haifeng Li. 2023. Self-supervised remote sensing feature learning: Learning paradigms, challenges, and future works. *IEEE Transactions on Geoscience and Remote Sensing* (2023).
- [68] Chao Tao, Ji Qi, Weipeng Lu, Hao Wang, and Haifeng Li. 2020. Remote sensing image scene classification with self-supervised paradigm under limited labeled samples. *IEEE Geoscience and Remote Sensing Letters* 19 (2020), 1–5.
- [69] Yonglong Tian, Dilip Krishnan, and Phillip Isola. 2020. Contrastive multiview coding. In *Computer Vision—ECCV 2020: 16th European Conference, Glasgow, UK, August 23–28, 2020, Proceedings, Part XI* 16. Springer, 776–794.
- [70] Naftali Tishby, Fernando C Pereira, and William Bialek. 2000. The information bottleneck method. *arXiv preprint physics/0004057* (2000).
- [71] Ilya Tolstikhin, Olivier Bousquet, Sylvain Gelly, and Bernhard Schölkopf. 2017. Wasserstein auto-encoders. *arXiv preprint arXiv:1711.01558* (2017).
- [72] Devis Tuia, Claudio Persello, and Lorenzo Bruzzone. 2016. Domain adaptation for the classification of remote sensing data: An overview of recent advances. *IEEE geoscience and remote sensing magazine* 4, 2 (2016), 41–57.
- [73] Vladimir N. Vapnik. 1998. *Statistical Learning Theory*. Wiley-Interscience.
- [74] Stefano Vincenzi, Angelo Porrello, Pietro Buzzega, Marco Cipriano, Pietro Fronte, Roberto Cucchi, Carla Ippoliti, Annamaria Conte, and Simone Calderara. 2021. The color out of space: learning self-supervised representations for earth observation imagery. In *2020 25th International Conference on Pattern Recognition (ICPR)*. IEEE, 3034–3041.
- [75] Oriol Vinyals, Alexander Toshev, Samy Bengio, and Dumitru Erhan. 2015. Show and tell: A neural image caption generator. In *Proceedings of the IEEE conference on computer vision and pattern recognition*. 3156–3164.
- [76] Riccardo Volpi, Hongseok Namkoong, Ozan Sener, John C Duchi, Vittorio Murino, and Silvio Savarese. 2018. Generalizing to unseen domains via adversarial data augmentation. *Advances in neural information processing systems* 31 (2018).
- [77] Yi Wang, Conrad M Albrecht, Nassim Ait Ali Braham, Lichao Mou, and Xiao Xiang Zhu. 2022. Self-supervised learning in remote sensing: A review. *arXiv preprint arXiv:2206.13188* (2022).
- [78] Zijian Wang, Yadan Luo, Ruihong Qiu, Zi Huang, and Mahsa Baktashmotlagh. 2021. Learning to diversify for single domain generalization. In *Proceedings of the IEEE/CVF International Conference on Computer Vision*. 834–843.
- [79] Qinwei Xu, Ruipeng Zhang, Yi-Yan Wu, Ya Zhang, Ning Liu, and Yanfeng Wang. 2023. SimDE: A Simple Domain Expansion Approach for Single-Source Domain Generalization. In *Proceedings of the IEEE/CVF Conference on Computer Vision and Pattern Recognition*. 4797–4807.
- [80] Qinwei Xu, Ruipeng Zhang, Ya Zhang, Yanfeng Wang, and Qi Tian. 2021. A fourier-based framework for domain generalization. In *Proceedings of the IEEE/CVF Conference on Computer Vision and Pattern Recognition*. 14383–14392.
- [81] Jure Zbontar, Li Jing, Ishan Misra, Yann LeCun, and Stéphane Deny. 2021. Barlow twins: Self-supervised learning via redundancy reduction. In *International Conference on Machine Learning*. PMLR, 12310–12320.
- [82] Xiaohua Zhai, Avital Oliver, Alexander Kolesnikov, and Lucas Beyer. 2019. S4L: Self-supervised semi-supervised learning. In *Proceedings of the IEEE/CVF international conference on computer vision*. 1476–1485.
- [83] Renrui Zhang, Rongyao Fang, Wei Zhang, Peng Gao, Kunchang Li, Jifeng Dai, Yu Qiao, and Hongsheng Li. 2021. Tip-adapter: Training-free clip-adapter for better vision-language modeling. *arXiv preprint arXiv:2111.03930* (2021).
- [84] Richard Zhang, Phillip Isola, and Alexei A Efros. 2017. Split-brain autoencoders: Unsupervised learning by cross-channel prediction. In *Proceedings of the IEEE conference on computer vision and pattern recognition*. 1058–1067.
- [85] Zhaoyang Zhang, Xuying Wang, Xiaoming Mei, Chao Tao, and Haifeng Li. 2022. FALSE: False Negative Samples Aware Contrastive Learning for Semantic Segmentation of High-Resolution Remote Sensing Image. *IEEE Geoscience and Remote Sensing Letters* 19 (2022), 1–5.
- [86] Long Zhao, Ting Liu, Xi Peng, and Dimitris Metaxas. 2020. Maximum-Entropy Adversarial Data Augmentation for Improved Generalization and Robustness. In *Advances in Neural Information Processing Systems*, H. Larochelle, M. Ranzato, R. Hadsell, M.F. Balcan, and H. Lin (Eds.), Vol. 33. Curran Associates, Inc., 14435–14447. https://proceedings.neurips.cc/paper_files/paper/2020/file/a5bfc9e07964f8dddeb95fc584cd965d-Paper.pdf
- [87] Juepeng Zheng, Wenzhao Wu, Shuai Yuan, Haohuan Fu, Weijia Li, and Le Yu. 2021. Multisource-domain generalization-based oil palm tree detection using very-high-resolution (vhr) satellite images. *IEEE Geoscience and Remote Sensing Letters* 19 (2021), 1–5.
- [88] Kaiyang Zhou, Jingkang Yang, Chen Change Loy, and Ziwei Liu. 2022. Conditional prompt learning for vision-language models. In *Proceedings of the IEEE/CVF Conference on Computer Vision and Pattern Recognition*. 16816–16825.
- [89] Kaiyang Zhou, Jingkang Yang, Chen Change Loy, and Ziwei Liu. 2022. Learning to prompt for vision-language models. *International Journal of Computer Vision* 130, 9 (2022), 2337–2348.
- [90] Kaiyang Zhou, Yongxin Yang, Timothy Hospedales, and Tao Xiang. 2020. Deep domain-adversarial image generation for domain generalisation. In *Proceedings of the AAAI Conference on Artificial Intelligence*, Vol. 34. 13025–13032.
- [91] Kaiyang Zhou, Yongxin Yang, Yu Qiao, and Tao Xiang. 2021. Domain generalization with mixstyle. *arXiv preprint arXiv:2104.02008* (2021).
- [92] Beier Zhu, Yulei Niu, Yucheng Han, Yue Wu, and Hanwang Zhang. 2022. Prompt-aligned Gradient for Prompt Tuning. *arXiv preprint arXiv:2205.14865* (2022).